Application of adaptive neuro-fuzzy inference system for prediction of dissolved oxygen concentration in the gold cyanide leaching process

Ali Behnamfard [a, *], Mohammad Rivaz [a]

[a] *Faculty of Engineering, University of Birjand, Birjand, South Khorasan, Iran.*

ABSTRACT

An adaptive neuro-fuzzy inference system (ANFIS) model has been developed for the prediction of the dissolved oxygen concentration (DOC) as a function of the solution temperature (0-40°C), salinity based on conductivity (0-59000 μS/cm), and atmospheric pressure (600-795 mmHg). The data set was randomly divided into two parts, training and testing sets. 80% of the data points (80% = 11556 datasets) were utilized for training the model and the remainder data points (20% =2889 datasets) were utilized for its testing. Several indices of performance such as root mean squared error (RMSE), mean absolute percentage error (MAPE), and coefficient of correlation (R) were used for checking the accuracy of data modeling. ANFIS models for the prediction of DOC were constructed with various types of membership functions (MFs). The model with the generalized bell MF had the best performance among all of the given models. The results indicate that ANFIS is a powerful tool for the accurate prediction of DOC in gold cyanidation tanks.

1. Introduction

Cyanidation is the dominant process for the extraction of gold from its ores due to the low cost and process simplicity compared to the other metallurgical methods [1]. This process includes the dissolution of gold from ores in dilute cyanide solutions in the presence of lime and oxygen [1-3]. One mole of gold requires half a mole of oxygen and two moles of cyanide for dissolution [1, 4]. The gold leaching rate greatly reduces when DOC drops below 4mg/L and increases considerably when the DOC is greater than 10mg/L [4]. DOC achievable in most gold cyanide leaching operations range from about 4mg/L to more than 15 mg/L based on atmospheric pressure, solution temperature, and salinity [1, 5]. Therefore, the prediction of DOC in the cyanidation tanks is essential in designing and controlling a cyanidation process.

Fuzzy logic is a powerful, yet straightforward, problem-solving technique that defines and generates responses based on ambiguous, qualitative, incomplete, and imprecise information, and fuzzy systems have fascinated the growing attention and interest in decision making studies, pattern recognition, quality control, and data analysis [6, 7]. A specific approach in neuro-fuzzy development is the adaptive neuro-fuzzy inference system (ANFIS), which has shown significant results in modeling non-linear functions. Many researchers reported the applicability of ANFIS in prediction purposes. Tutmez used ANFIS for the modeling of the electrical conductivity of groundwater [8]. Behnamfard and Alaei predicted the coal proximate analysis factors and coal calorific value by ANFIS [9]. Behnamfard and Veglio studied the applicability of ANFIS for the prediction of xanthate decomposition percentage as a function of pH, temperature, and time [10]. Jalalifar et al. applied ANFIS for the prediction of a rock engineering classification system [11].

The dissolution rate of gold in alkaline cyanide solutions under atmospheric conditions, and at practical cyanide levels, is directly proportional to DOC. The oxygen improves gold dissolution kinetics, reducing residence time and increasing plant throughput. Furthermore, the cyanide addition reduces 25% by using oxygen rather than air in the process. The effects of DOC on gold dissolution and cyanide consumption also depend on the characteristics of the ore under consideration. In the case of refractory gold ores, some sulfide minerals, in particular pyrite, react with the cyanide causing additional reagent consumption. Therefore, the prediction of DOC in the cyanidation pulp can be effective in the design and control of the gold cyanidation process. In this research, ANFIS as a powerful tool in fuzzy modeling and prediction purposes has been used for the prediction of DOC which has not received any attention up to now.

2. Methodology

2.1. Adaptive neuro-fuzzy inference system (ANFIS)

ANFIS is a kind of artificial neural network that is based on the Takagi Sugeno fuzzy inference system that was first introduced by Jang in 1993 [12]. Since it gathered both fuzzy logic and neural network principles, it has the potential to get the benefits of both in a single framework. Its inference system corresponds to a set of fuzzy If–then rules that have the learning capability to approximate nonlinear systems [12-14].

To describe the ANFIS system, it is simply surmised that the inference system has two inputs x and y, and one output f. A first-order Sugeno fuzzy model has rules as the following:

Rule 1. If x is A_1 and y is B_1, then $f_1 = p_1x + q_1y + r_1$.
Rule 2. If x is A_2 and y is B_2, then $f_2 = p_2x + q_2y + r_2$.

where p_1, p_2, q_1, q_2, r_1, and r_2 are linear parameters in the consequent part, and A_1, A_2, B_1, and B_2 are nonlinear parameters.

Figure 1 illustrates the corresponding equivalent ANFIS architecture for two input first-order Sugeno fuzzy models with two rules. The entire

---

* Corresponding author. Tel: +98 56 3102 6473, *E-mail address: behnamfard@birjand.ac.ir* (A. Behnamfard).

system architecture consists of five layers, namely the fuzzy layer, product layer, normalized layer, de-fuzzy layer, and total output layer [15-22]. The node functions in the same layer are of the same function family as described in the following:

Layer 1: This layer is called the fuzzy layer. The adjustable nodes in this layer are represented by square nodes and marked by A_1, A_2, B_1, and B_2 with x and y outputs. A_1, A_2, B_1, and B_2 are the linguistic labels (small, large, etc.) used in the fuzzy theory for dividing the MFs. The node functions in this layer that determines the membership relation between the input and output functions can be given by:

$$O_{1,i} = \mu_{A_i}(x), i = 1, 2 \quad , \quad O_{1,j} = \mu_{B_j}(y), j = 1, 2 \tag{1}$$

where $O_{1,i}$ and $O_{1,j}$ denote the output functions, and μ_{Ai} and μ_{Bj} denote the appropriate MFs, which could be triangular, trapezoidal, Gaussian functions, or other shapes.

Layer 2: this is the product layer and every node is a fixed node marked by a circle node and labeled by Prod. The outputs w_1 and w_2 are the weight functions of the next layer. The output of this layer, $O_{2,i}$, is the product of all the incomings signals and given by:

$$O_{2,i} = w_i = \mu_{A_i}(x)\,\mu_{B_i}(y), i = 1, 2 \tag{2}$$

The output signal of each node, w_i, represents the firing strength of a rule.

Layer 3: this is the normalized layer and every node in this layer is a fixed node, marked by a circle node and labeled by Norm. The nodes normalize the firing strength by estimating the ratio of firing strength for this node to the sum of all the firing strengths, i.e.

$$O_{3,i} = \overline{w_i} = \frac{w_i}{w_1 + w_2}, i = 1, 2 \tag{3}$$

Layer 4: this is the de-fuzzy layer having adaptive nodes and marked by square nodes. Every node i in this layer is an adaptive node with a node function:

$$O_{4,i} = \overline{w_i} f_i = \overline{w_i}\,(p_i x + q_i y + r_i), i = 1, 2 \tag{4}$$

where $\overline{w_i}$ is the normalized firing strength output from layer 3 and p_i, q_i and r_i are the parameters set of this node. These parameters are linear and referred to as consequent parameters of this node.

Layer 5: The single node in this layer is a fixed node marked by circle node and labeled sum, which computes the overall output as the summation of all incoming signals:

$$O_{5,i} = \sum_{i=1}^{2} \overline{w_i}\, f_i = \frac{\sum_{i=1}^{2} w_i f_i}{w_1 + w_2} \tag{5}$$

The number of fuzzy sets is determined by the number of nodes in the first layer. On the other hand, the number of layer 4 dimensions indicates the number of fuzzy rules employed in the architecture that shows the complexity and flexibility of the ANFIS architecture. Fuzzy rules can be considered as the equivalent of the neurons when compared to the neural networks.

An ANFIS network can be trained based on supervised learning to reach from a specific input to the particular target output. In the forward pass of the hybrid algorithm of the ANFIS, the node outputs go forward until the fourth layer and consequent linear parameters, (p_i, q_i, r_i), are found by the least-squares method using training data. The error signals propagate backward in the backward pass and the premise nonlinear parameters, (a_i, b_i, c_i), are updated by gradient descent. It has been proven that this hybrid algorithm is highly efficient in training the ANFIS [15-22].

2.2. Development of ANFIS models

As can be seen in Figure 2, the ANFIS model based on a grid partitioning algorithm with three inputs (i.e., solution temperature, salinity based on conductivity, and atmospheric pressure) and one output (i.e., DOC) was designed to predict DOC. Data used in this paper for ANFIS modeling were obtained from the report of the United States Geological Survey (USGS) about techniques of water-resources investigations [5]. This report presents DOC as a function of solution temperature, atmospheric pressure, and solution conductivity. The description of the input and output parameters in the ANFIS model is reported in Table 1.
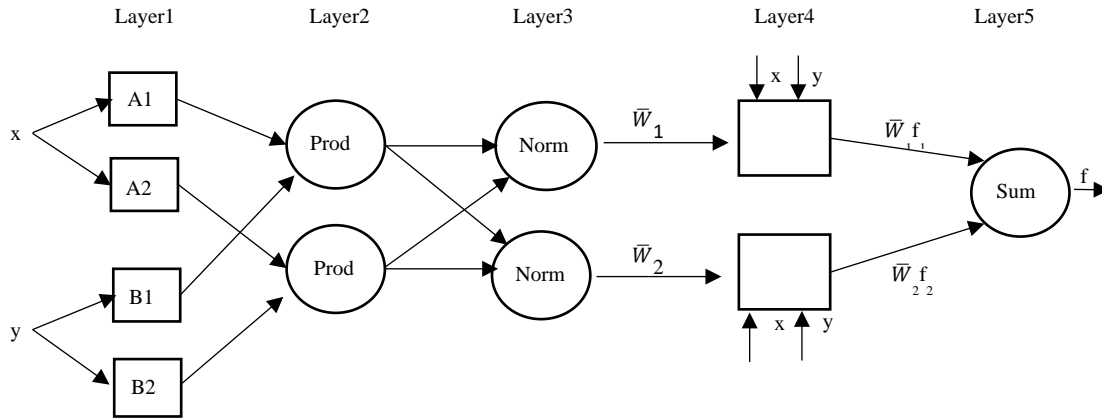

Figure 1. An ANFIS network structure for a simple FIS.

Table 1. Description of the input and output parameters in ANFIS.

Parameter	Description	Symbol	Range	Mean	Variance
Input	atmospheric pressure	pressure	600-795 mmHg	699.2503	66.3232
	Salinity based solution conductivity	conductivity	0-59000μS/cm	26471.37	18690.32
	solution temperature	temperature	0-40ºC	17.79713	10.58042
Output	Dissolved oxygen concentration	DOC	4.36698-15.3	8.240149	2.073009

The data set was randomly divided into two parts, training and testing sets. 80% of the data points (80%=11556 datasets) were utilized for training the model and the remainder data points (20% =2889 datasets) were utilized for its testing. The domain of each antecedent variable is partitioned into equidistant and identically shaped MFs in the grid partitioning method. The total number of fuzzy rules (S_{total}) increase

exponentially with the input dimension, i.e., $S_{total} = M_n$ where n is the input dimension, and M is the number of partitioned fuzzy subsets for each input variable. It is clear that for this type of partition the number of fuzzy rules will increase exponentially with the number of input dimensions, so the number of rules will be huge when the number of input dimensions is large and a lot of computations are needed.
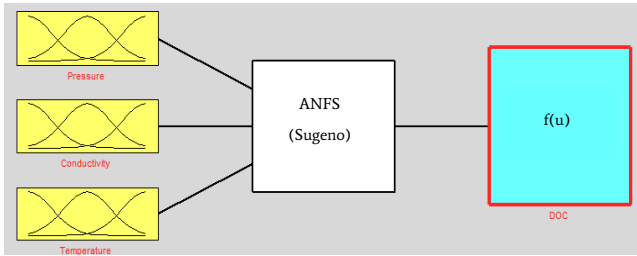
Figure 2. System ANFIS: 3 inputs (pressure, conductivity, and temperature), 1 output (DOC).

2.3. Definition of MFs

In this research, the ANFIS models have been constructed by using four different MFs including triangular, trapezoidal, Gaussian, and generalized bell MFs. The MFs are defined as follows:

A triangular MF is specified by three parameters {a, b, c} as follows [23]:

$$\mu_A(x) = \begin{cases} 0, x \le a. \\ \frac{x-a}{b-a}, a \le x \le b \\ \frac{c-x}{c-b}, b \le x \le c \\ 0, c \le x. \end{cases} \tag{6}$$

The parameters {a, b, c} (with a < b < c) determine the x coordinates of the three corners of the underlying triangular MF. Figure 3a shows a triangular MF defined by a triangle (x; 20, 60, 80).

A trapezoidal MF is specified by four parameters {a, b, c, d} as follows [23]:

$$\mu_A(x) = \begin{cases} 0, \ x \le a. \\ \frac{x-a}{b-a}, \ a \le x \le b \\ 1, b \le x \le c \\ \frac{d-x}{d-c}, \ c \le x \le d. \\ 0, \ d \le x. \end{cases} \tag{7}$$

The parameters {a, b, c, d} (with a < b <= c < d) determine the x coordinates of the four corners of the underlying trapezoidal MF. Figure 3b shows a trapezoidal MF defined by trapezoid (x; 10, 20, 60, 95).

A Gaussian MF is specified by two parameters as follows [23]:

$$\mu_A(x) = exp(-\frac{(x-c)^2}{2\sigma^2}) \tag{8}$$

A Gaussian MF is determined completely by c and σ; c represents the MFs center and σ determines the MFs width. Figure 3c plots a Gaussian MF defined by Gaussian (x; 50, 20).

A generalized bell MF is specified by three parameters {a, b, c} as follows [23]:

$$\mu_A(x) = \frac{1}{1+\left(\frac{x-c}{a}\right)^{2b}} \tag{9}$$

where the parameter b is usually positive. Figure 3d shows a generalized bell MF defined by a bell (x; 20, 40, 50).

2.4. Validation of the ANFIS models

The applicability of ANFIS models to predict DOC was validated by the following criteria:

Root mean squared error (RMSE) [24]:

$$RMSE = \sqrt{\frac{1}{N}\sum_{t=1}^{N}(A_t - F_t)^2} \tag{10}$$

where A_t and F_t are actual and predicted values, respectively, and N is the number of training or testing samples.

Mean absolute percentage error (MAPE) [24]:

$$MAPE = \frac{1}{N}\sum_{t=1}^{N}\left|\frac{A_t-F_t}{A_t}\right| \times 100 \tag{11}$$

Correlation coefficient (R) [24]:

$$R = \frac{\sum_{t=1}^{N}(A_t-\overline{A})(F_t-\overline{F})}{\sqrt{\sum_{t=1}^{n}(A_t-\overline{A})^2 . \sum_{t=1}^{n}(F_t-\overline{F})^2}} \tag{12}$$

Where $\overline{A} = \frac{1}{N}\sum_{t=1}^{N}A_t$ and $\overline{F} = \frac{1}{N}\sum_{t=1}^{N}F_t$ are the average values of A_t and F_t over the training or testing dataset. The smaller RMSE and MAPE and larger R mean better performance.
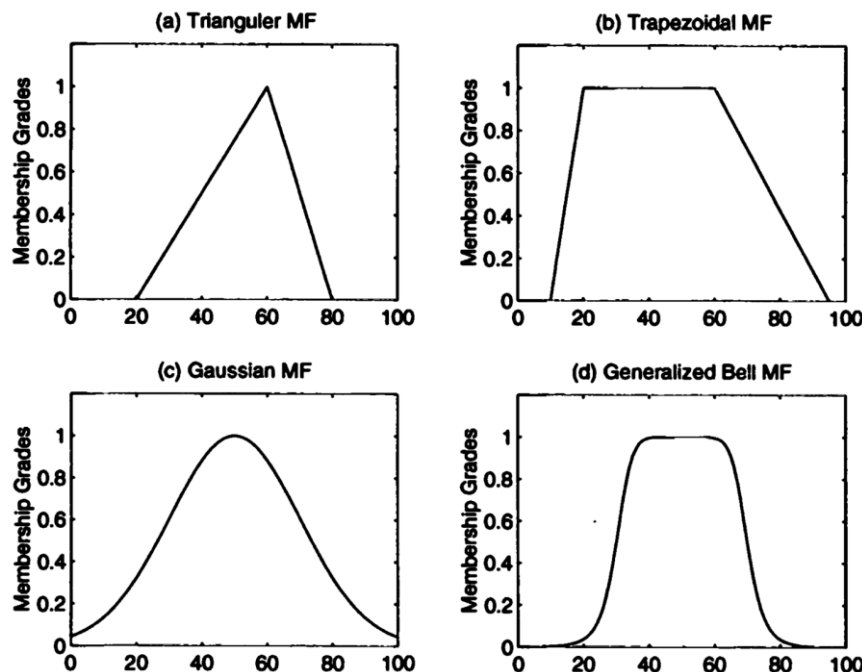

Figure 3. Illustration of four types of parameterized MFs: (a) triangle (x; 20, 60, 80); (b) trapezoid (x; 10, 20, 60, 95); (c) Gaussian (x; 50, 20) and (d) bell (x; 20, 40, 50)[23].

3. Results and Discussion

In this research, a hybrid grid partitioning ANFIS by four different MFs including triangular, trapezoidal, Gaussian, and generalized bell MFs was applied in order to predict DOC as a function of atmospheric pressure, solution temperature, and solution conductivity. Figure 4 shows the model structure of the ANFIS that is to be built for DOC prediction in this study. Also, the characterizations of ANFIS models are shown in Table 2.

Figure 5 shows the effect of solution temperature and atmospheric pressure on DOC. It can be seen that DOC decreases with increasing solution temperature. For example, DOCs at a solution temperature of 0 and 40^OC, the atmospheric pressure of 760 mmHg, and conductivity of 0μS/cm are 14.62 and 6.41 mg/L, respectively. Figure 5 also shows that DOC increases with increasing atmospheric pressure. For example, DOCs at atmospheric pressure of 600 and 795 mmHg, solution temperature of 25^OC, and conductivity of 0μS/cm are 6.47 and 8.66 mg/L, respectively.
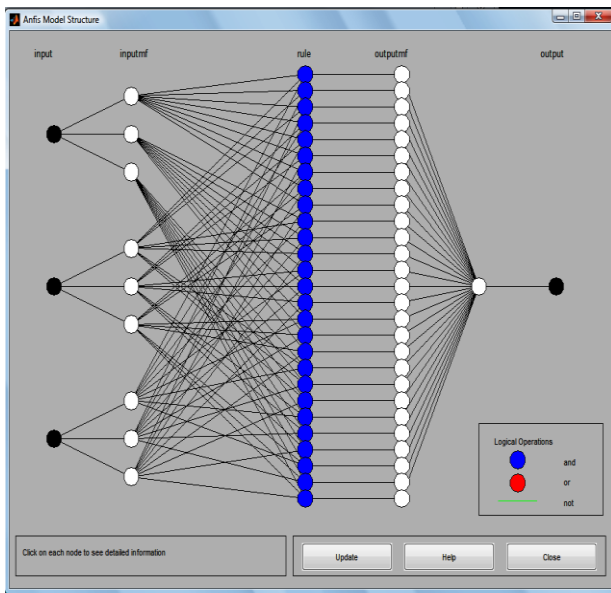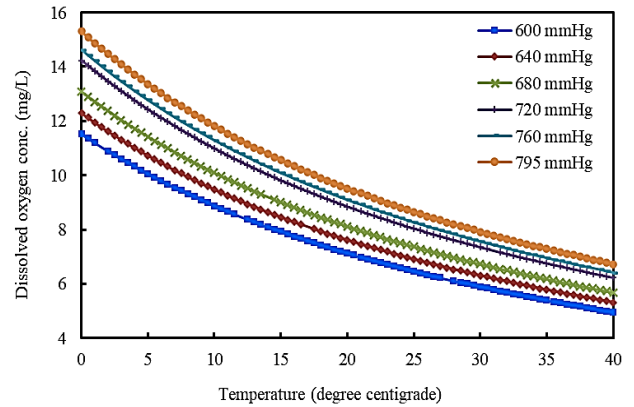

Figure 5. The effect of solution temperature and atmospheric pressure on DOC at solution conductivity of 0μS/cm.

Figure 6 shows the effect of solution temperature and conductivity on DOC at atmospheric pressure of 760 mmHg. It can be seen that DOC decreases with increasing solution conductivity at various solution temperatures. This figure also indicates that the effect of solution conductivity on DOC is more significant at lower solution temperatures. The ANFIS models by using various MFs are compared based on their performance in training data sets and testing data sets. All three indices including RMSE, MAPE, and correlation coefficients (R), processed with a different types of MFs, are listed in Table 3 for comparison purposes. It appears that the ANFIS models by various MFs are accurate and consistent, where all of the RMSE and MAPE values have near-zero values, and all of the correlation coefficients (R) are very close to unity. Nonetheless, the best prediction of DOC was obtained when using Generalized bell MF. The shape of the membership function can be influenced the computational complexity and accuracy of the designed ANFIS-based model [25-27]. Nevertheless, the shape of the membership function has more influence on the computational complexity and at a high number of the epoch, there is no significant difference between various membership functions [25-27]. As can be seen in Table 2, there is a difference between the number of epochs for obtaining the best results by using various membership functions. On the other hand, the applicability of ANFIS for the data used in this research is good regardless of the type of membership function. In some cases, data variation is high and it affects the ANFIS performance.

Figure 4. Model structure of the ANFIS for DOC prediction.

Table 2. Different parameter types and their values used for training ANFIS models.

ANFIS parameter type	Membership Function Type			
	Gaussian	Triangular	trapezoidal	Generalized bell
Number of MFs	3 3 3	3 3 3	3 3 3	3 3 3
Output MF	Linear	Linear	Linear	Linear
Number of nods	78	78	78	78
Number of linear parameters	108	108	108	108
Number of nonlinear parameters	18	27	36	27
Total number of parameters	126	135	144	135
Number of training data pairs	11556	11556	11556	11556
Number of testing data pairs	2889	2889	2889	2889
Number of fuzzy rules	27	27	27	27
Number of epoch	1500	200	1500	350

Figure 7 shows the applicability of the ANFIS model by Generalized bell MF to predict DOC at various solution temperatures, atmospheric pressures, and solution conductivities. As can be seen, the ANFIS model maintains its excellent prediction accuracy throughout the range of DOC, hence showing consistency and a high degree of generalization capability.

Figure 8 shows the initial (before training) and final (after training)

MFs of the three input parameters using the Gaussian MF. This analysis was performed since the number of changes in the final MFs of inputs indicates the impact of inputs on the detection of output. Based on the analysis of MFs, it can be seen that temperature has the most important effect on the final MF. It may be due to the effect of temperature, pressure, and conductivity on DOC. The temperature has a more significant effect on the DOC rather than pressure and conductivity.

Table 3. Performances of ANFIS models by different MFs in the prediction of DOC.

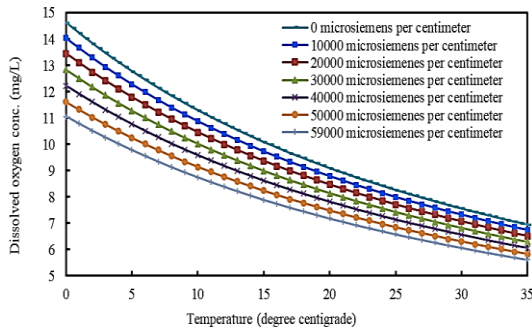| Membership function	Training dataset			Testing dataset		
	RMSE	MAPE (%)	R	RMSE	MAPE (%)	R
Gaussian	1.58991E-05	0.039396	0.999998	1.56204E-05	0.039495	0.999998
Triangular	9.28579E-05	0.080979	0.999989	9.50142E-05	0.079677	0.999989
Trapezoidal	3.04254E-05	0.0532	0.999996	3.28121E-05	0.054862	0.999996
Generalized bell	1.6578E-05	0.040237	0.999998	1.49734E-05	0.038882	0.999998

Figure 6. The effect of solution temperature and conductivity on DOC at atmospheric pressure of 760 mmHg.
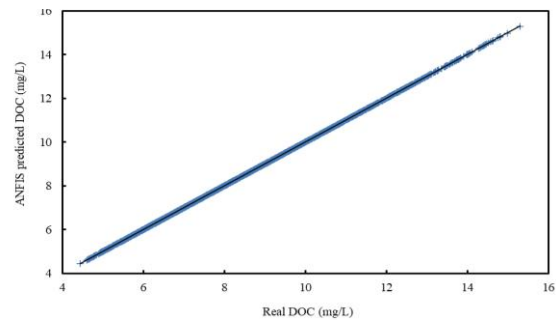

Figure 7. Predicted DOCs with ANFIS at various solution temperatures (0-40°C), atmospheric pressures (600-795 mmHg) and solution conductivities (0-59000µS/cm) vs. real DOCs.
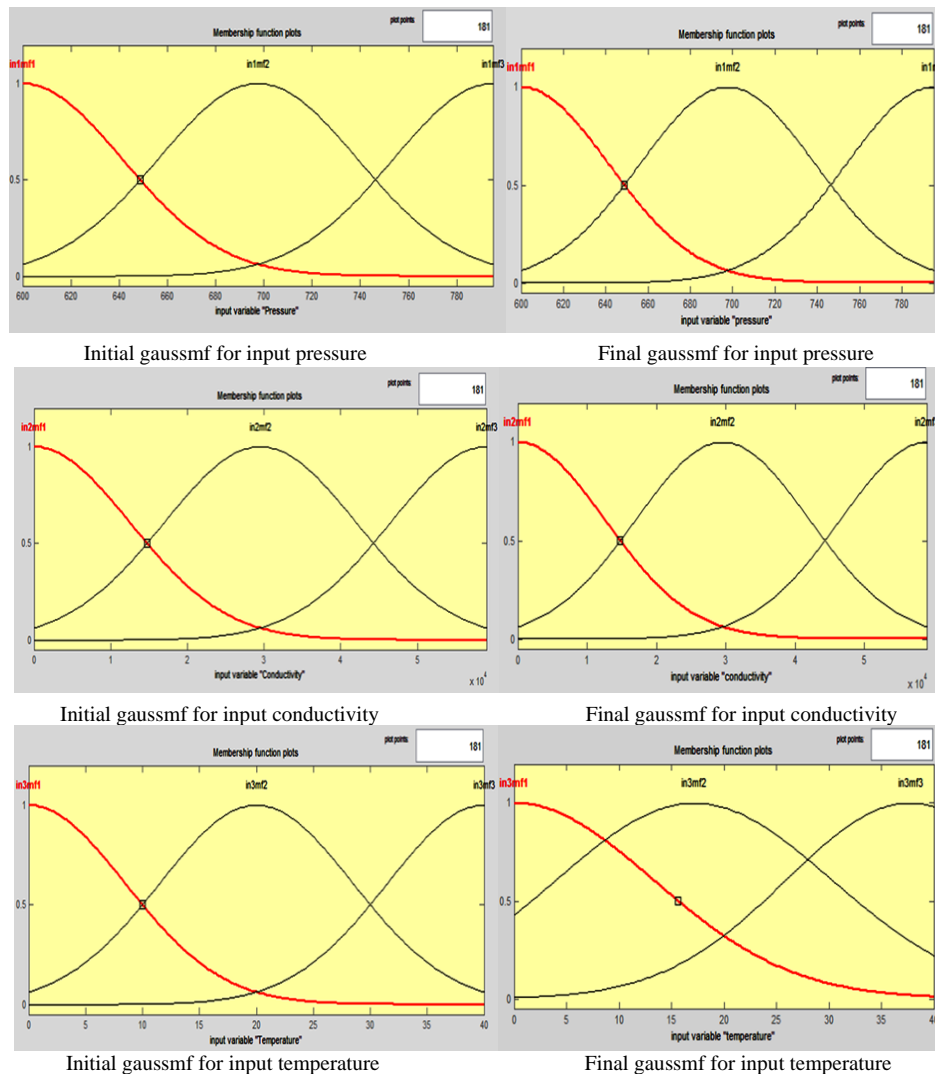

Initial gaussmf for input pressure

Final gaussmf for input pressure

Initial gaussmf for input conductivity

Final gaussmf for input conductivity

Initial gaussmf for input temperature

Final gaussmf for input temperature

Figure 8. The Gaussian MFs before and after training.

Figure 9 shows the initial and final MFs of the three input parameters using the generalized bell MF. The examination of initial and final MFs indicates that there is a considerable change in the final MFs of one input parameter namely temperature. Analysis of these figures indicates that the temperature as an input parameter has a considerable effect on the final MF. It may be due to the effect of temperature, pressure, and conductivity on DOC. The temperature has a more significant effect on the DOC rather than pressure and conductivity

Figure 10 shows the final rules of the fuzzy inference system by using generalized bell MFs. The fourth column of this figure shows the location (firing magnitude) of the rules at the end of the training. For each of the inputs, three bell-shaped MFs were selected. These three MFs were designed to cluster the input space of each variable into three overlapping segments—low, medium, and high. The trained if-then rules can be used for prediction. In other words, if we change the values of the three inputs, then we immediately get the new output value of the ANFIS.

Once the system is trained, one can examine the input/output relationships, in an illustrative manner. Figure 11 illustrates the response of the system when two variables are changed, and the third variable is fixed at its mean value. Figure 11a indicates that the temperature has a more important effect on DOC than pressure. Figure 11b shows that the DOC increases in a constant manner by increasing pressure and decreasing conductivity. Figure 11c shows that temperature has a higher predictive power on DOC, as compared to the conductivity.
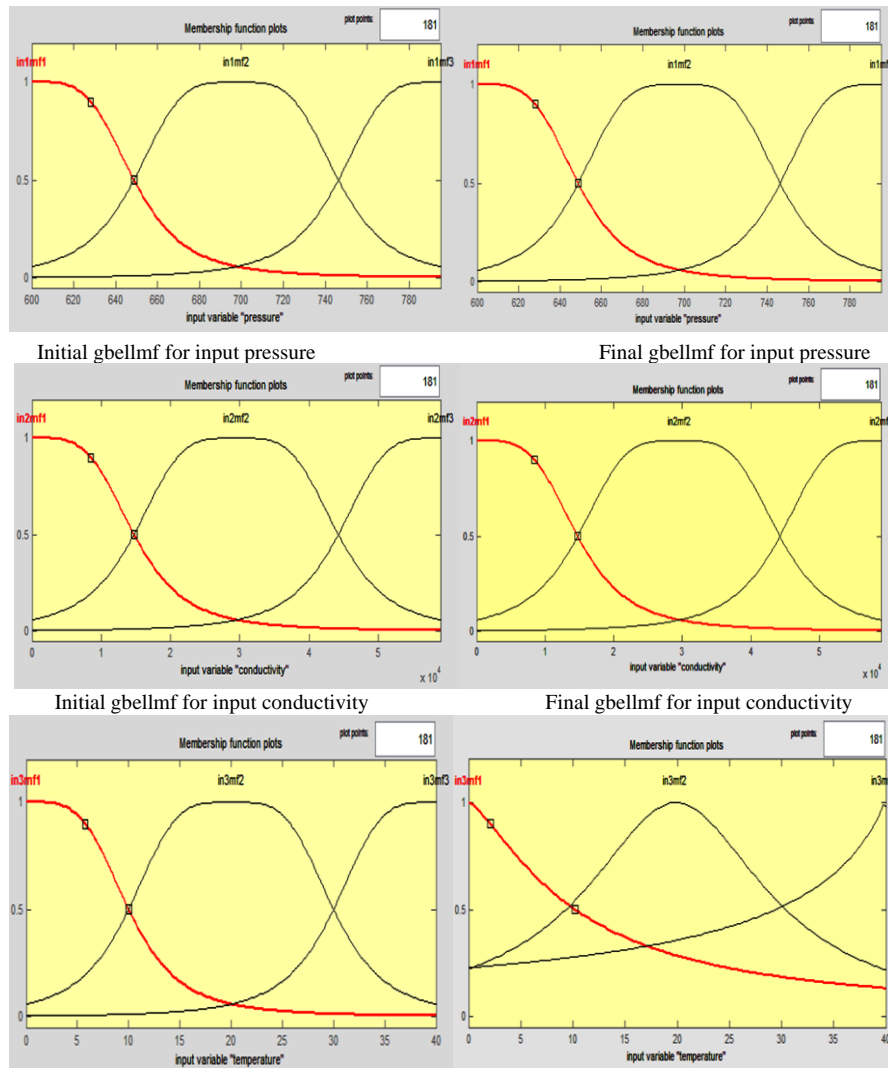

Initial gbellmf for input pressure　　　　　Final gbellmf for input pressure

Initial gbellmf for input conductivity　　　　　Final gbellmf for input conductivity

Figure 9. The Generalized bell MFs before and after training.

4. Conclusion

We presented a new application of the ANFIS for the prediction of DOC as a function of solution temperature, salinity based on conductivity, and pressure. The ANFIS models are very powerful to build a complex and nonlinear relationship between inputs and outputs by learning among a set of given data. Since the ANFIS models have high accuracy and require no complicated mathematical functions, they can be very useful for the development of fast models.

Four different ANFIS models were developed, each one of them based on a different type of membership function: a Gaussian, a generalized bell, a trapezoidal, and a triangular membership function. The investigation revealed that ANFIS modeling accuracy is not considerably affected by the type of membership function employed. The ANFIS model with generalized bell membership function was qualified as the most accurate among the examined cases.

The values of RMSE, MAPE, and R values for training and testing data sets by using generalized bell membership function were 1.66×10^{-5}, 0.04, 1 and 1.5×10^{-5}, 0.039, and 1, respectively. The temperature has the most important effect on the final membership function among the other variables. Finally, the user can accurately and conveniently obtain the DOC by GUI.
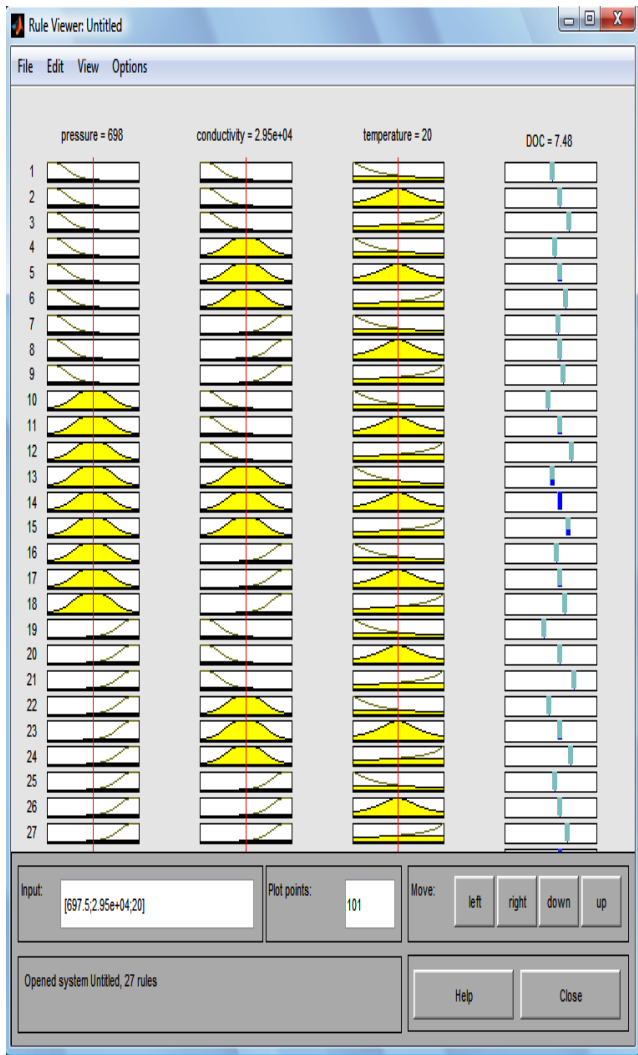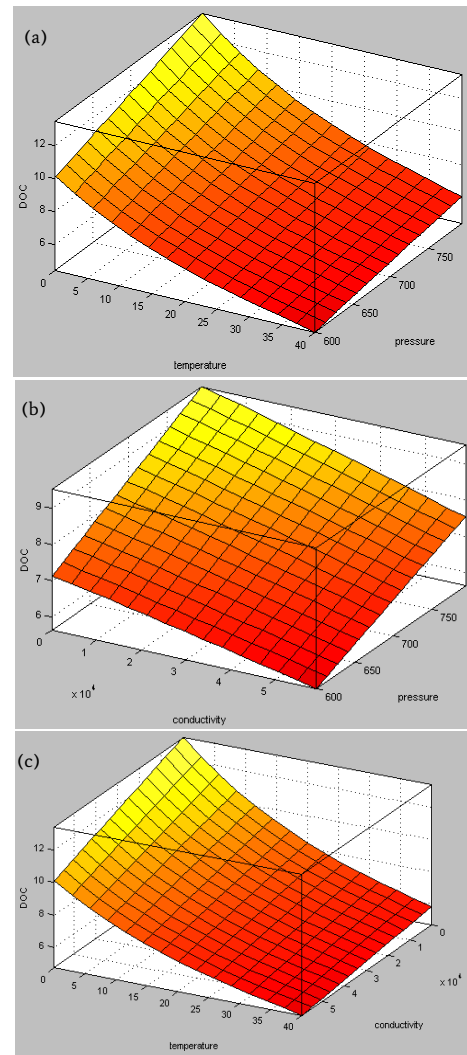
Figure 10. If–then rules after training.

Figure 11. (a) DOC vs. (temperature and pressure); (b) DOC vs. (conductivity and pressure); (c) DOC vs. (temperature and conductivity).

References

[1] Marsden, J. O., House, C. I. (2006). The chemistry of gold extraction. second ed., Society for mining, metallurgy, and exploration, Colorado, USA.

[2] Salarirad, M. M., & Behnamfard, A. (2010). The effect of flotation reagents on cyanidation, loading capacity and sorption kinetics of gold onto activated carbon. Hydrometallurgy, 105 (1-2), 47-53.

[3] Behnamfard, A., Chegni, K., Alaei, R., & Veglio, F. (2019). The effect of thermal and acid treatment of kaolin on its ability for cyanide removal from aqueous solutions. Environmental Earth Sciences, 78(14), 1-12.

[4] Deschenes, G. (2005). Technological development in the cyanidation of gold. Proceeding of the Canadian mineral processors, Canada.

[5] Rounds, S. A., Wilde, F.D., Ritz, G. F. (2013). Dissolved oxygen. Book 9, chap. A6, sec. 6.2, U.S. Geological Survey Techniques of Water-Resources Investigations, USA.

[6] Buyukbingol, E., Sisman, A., Akyildiz, M., Alparslan, F. N., Adejare, A. (2007). Adaptive neuro-fuzzy inference system (ANFIS): A new approach to predictive modeling in QSAR applications: A study of neuro-fuzzy modeling of PCP-based NMDA receptor antagonists. Bioorganic and Medicinal Chemistry,15, 4265–4282.

[7] Pan, L., Yang, S. X. (2007). Analysing livestock farm odour using an adaptive neuro-fuzzy approach. Biosystems Engineering, 97, 387 – 393.

[8] Tutmez, B., Hatipoglu, Z., Kaymak, U. (2006). Modelling electrical conductivity of groundwater using an adaptive neuro-fuzzy inference system. Computational Geosciences, 32, 421–433.

[9] Behnamfard, A., Alaei, R. (2017). Estimation of coal proximate analysis factors and calorific value by multivariable regression method and adaptive neuro-fuzzy inference system (ANFIS). International Journal of Mining and Geo-Engineering, 51(1), 29-35.

[10] Behnamfard, A., Veglio, F. (2019). Estimation of xanthate decomposition percentage as a function of pH, temperature and time by least squares regression and adaptive neuro-fuzzy inference system. International Journal of Mining and Geo-Engineering, 53(2), 157-163.

[11] Jalalifar, H., Mojedifar, S., Sahebi, A. A., Nezamabadi-pour, H.

(2011). Application of the adaptive neuro-fuzzy inference system for prediction of a rock engineering classification system. Computers and Geotechnics, 38, 783–790.

[12] Jang, J. (1993). ANFIS: Adaptive network-based fuzzy inference systems. IEEE Transactions on Systems, Man, and Cybernetics, 23, 665-683.

[13] Ghoush, M. A., Samhouri, M., Al-Holy, M., Herald, T. (2008). Formulation and fuzzy modeling of emulsion stability and viscosity of a gum–protein emulsifier in a model mayonnaise system. Journal of Food Engineering, 84, 348–357.

[14] Qin, H., Yang, S. X. (2007). Adaptive neuro-fuzzy inference systems based approach to nonlinear noise cancellation for images. Fuzzy Sets and Systems, 158, 1036 − 1063.

[15] Rebouh, S., Bouhedda, M., Hanini, S. (2016). Neuro-fuzzy modeling of Cu(II) and Cr(VI) adsorption from aqueous solution by wheat straw. Desalination and Water Treatment, 57(14), 6515-6530.

[16] Roohian, H., Abbasi, A., Hosseini, Z., Jahanmiri, A. (2014). Comparative Modeling and analysis of the mass transfer coefficient in a turbulent bed contactor using artificial neural network and adaptive neuro-fuzzy inference systems. Separation Science and Technology, 49(10), 1574-1583.

[17] Shu, C., Ouarda, T. B. M. J. (2008). Regional flood frequency analysis at ungauged sites using the adaptive neuro-fuzzy inference system. Journal of Hydrology, 349, 31– 43.

[18] Wu, G. D., Lo, S. L. (2008). Predicting real-time coagulant dosage in water treatment by artificial neural networks and adaptive network-based fuzzy inference system. Engineering Applications of Artificial Intelligence, 21, 1189– 1195.

[19] Ubeyli, E. D., Guler, I. (2006). Adaptive neuro-fuzzy inference system to compute quasi-TEM characteristic parameters of micro shield lines with practical cavity sidewall profiles. Neurocomputing, 70, 296–304.

[20] Zubaidi, S. L., Al-Bugharbee, H., Ortega-Martorell, S., Gharghan, S. K., Olier, I., Hashim, K. S., Al-Bdairi, N. S. S., Kot, P. (2020). A novel methodology for prediction urban water demand by wavelet denoising and adaptive neuro-fuzzy inference system approach. Water, 12(6), 1628.

[21] Zeinalnezhad, M., Chofreh, A. G., Goni, F. A., & Klemeš, J. J. (2020). Air pollution prediction using semi-experimental regression model and Adaptive Neuro-Fuzzy Inference System. Journal of Cleaner Production, 261, 121218.

[22] Shariati, M., Mafipour, M. S., Haido, J. H., Yousif, S. T., Toghroli, A., Trung, N. T., & Shariati, A. (2020). Identification of the most influencing parameters on the properties of corroded concrete beams using an Adaptive Neuro-Fuzzy Inference System (ANFIS). Steel Compos Struct, 34(1), 155.

[23] Jang, J.S.R. (1997). Chapter2: Fuzzy Sets. In: Jang, J.S.R., Sun, C.T., Mizutani, E. (Eds.). Neuro-fuzzy and soft computing: a computational approach to learning and machine intelligence. USA: Prentice-Hall Upper Saddle River, pp. 24-28. Available at: http://www.soukalfi.edu.sk/01_NeuroFuzzyApproach.pdf

[24] Aqil, M., Kita, I., Yano, A., & Nishiyama, S. (2007). A comparative study of artificial neural networks and neuro-fuzzy in continuous modeling of the daily and hourly behaviour of runoff. Journal of hydrology, 337(1-2), 22-34.

[25] Surajudeen-Bakinde, N., Faruk, N., Oloyede, A., Abdulkarim, A., Olawoyin, L., Popoola, S., & Adetiba, E. (2021). Effect of Membership Functions and Data Size on the Performance of ANFIS-Based Model for Predicting Path Losses in the VHF and

UHF Bands. Journal of Engineering Research, 10(1A), 203-226. Available at: https://kuwaitjournals.org/jer/index.php/JER/article/view/10457

[26] Ali, O.A.M., Ali, A.Y., & Sumait, B.S. (2015). Comparison between the effects of different types of membership functions on fuzzy logic controller performance. International Journal of Emerging Engineering Research and Technology, 3(3), 76-83.

[27] Talpur, N., Salleh, M. N. M., & Hussain, K. (2017). An investigation of membership functions on performance of ANFIS for solving classification problems. In: IOP Conference Series: Materials Science and Engineering, 226(1), 1-7. Available at:https://iopscience.iop.org/article/10.1088/1757899X/226/1/012103/pdf